

J. Sharma
H.B. Bohidar

Quasielastic light scattering study of chemically crosslinked gelatin solutions and gels

Received: 25 May 1999
Accepted in revised form: 27 July 1999

J. Sharma¹ · H.B. Bohidar (✉)
School of Physical Sciences
Jawaharlal Nehru University
New Delhi 110 067, India
e-mail: bohidar@jnuniv.ernet.in

Present address:
¹ Department of Chemistry
Indiana University-Purdue University
Indianapolis, IN 46202, USA

Abstract Quasielastic light scattering measurements are reported for experiments performed on mixtures of gelatin and glutaraldehyde (GA) in the aqueous phase, where the gelatin concentration was fixed at 5% (w/v) and the GA concentration was varied from 1×10^{-5} to 1×10^{-3} % (w/v). The dynamic structure factor, $S(q, t)$, was deduced from the measured intensity autocorrelation function, $g_2(\tau)$, with appropriate allowance for heterodyning detection in the gel phase. The $S(q, t)$ data could be fitted to $S(q, t) = A \exp(-D_f q^2 t) + B \exp(-t/\tau_c)^\beta$, both in the sol (50 and 60 °C) and gel states (25 and 40 °C). The fast-mode diffusion coefficient, D_f showed almost negligible dependence on the concentration of the crosslinker GA; however, the resultant mesh size, ξ , of the crosslinked network exhibited

strong temperature dependence, $\xi \sim (0.5 - \chi)^{1/5} \exp(-A/RT)$ implying shrinkage of the network as the gel phase was approached. The slow-mode relaxation was characterized by the stretched exponential factor $\exp(-t/\tau_c)^\beta$. β was found to be independent of GA concentration but strongly dependent on the temperature as $\beta = \beta_0 + \beta_1 T + \beta_2 T^2$. The slow-mode relaxation time, τ_c , exhibited a maximum GA concentration dependence in the gel phase and at a given temperature we found $\tau_c(c) = \tau_0 + \tau_1 c + \tau_2 c^2$. Our results agree with the predictions of the Zimm model in the gel case but differ significantly for the sol state.

Key words Quasielastic light scattering studies · Gelatin gels · Chemical crosslinking · Fast and slow modes

Introduction

Gelatin, which is denatured collagen, forms physical gels in hydrogen-bond-friendly solvents below a temperature of about 30 °C, at a relatively low gelatin concentration (about 2% w/v) in aqueous solutions [1–4]. In the gel phase, a three-dimensional interconnected network of polymer chains is formed in the dispersion medium. In the case of gelatin, the physically intertwined triple helices provide the junction zones to the network [5, 6]. The kinetics and thermodynamics of the gel transition for this polypeptide is rather well studied and documented [7–9]. The relaxation features measured by the dynamic

light scattering technique showed relaxation dynamics in both sol and gel states of this biopolymer often indicating anomalous diffusion behaviour. Amis et al. [10, 11] reported quasielastic light scattering (QELS) measurements on gelatin dissolved in water at concentrations above the overlap concentration, and observed two relaxation modes. The fast mode was attributed to cooperative diffusion and the slow mode was proposed to arise out of a self-diffusion process. Independent studies of the self-diffusion process performed by Brown et al. [12] and Chang and Yu [13] proved that the contention of self-diffusion giving rise to slow-mode relaxation was incorrect. Borsali et al. [14] and Herning

et al. [2] also measured fast (D_f) and slow diffusion (D_s) coefficients in the sol phase; the slow mode was reported to cease to exist at the onset of gelation [14].

Recent experiments have shown yet another mode, the intermediate mode, to exist along with the fast and slow modes both in the sol and gel states of gelatin solutions [15–17]. When a crosslinker such as glutaraldehyde (GA) is added to a gelatin solution there is a possibility that both physical and chemical crosslinking can coexist. Oikawa and Nakanishi [18] observed that the fast-mode diffusivity, D_f , is proportional to $c^{0.79}$, c being the gelatin concentration, but that the correlation length (mesh size) of the slow mode remained independent of c . Based on the static and dynamic light scattering data they concluded that the presence of GA did not alter the size of the crystalline triple-helical structures but depressed the number of nucleation sites, thus lowering the total crosslinking density.

In this work, we report dynamic structure factor, $S(q, t)$, measurements on GA cured gelatin solutions and gels at various concentrations of the crosslinker. The objective was to physically discriminate between the purely physically crosslinked gelatin gels and those of multi-ply crosslinked gels, where both physical and chemical crosslinks are present. In order to explore this further, we performed QELS experiments at various temperatures spanning the entire sol and gel phase of the system. The effect of heterodyne contribution to the structure factor data in the gel state, which is often neglected, has been accounted for in these measurements.

Experimental procedure

Materials and methods

Commercially obtained gelatin (bovine origin) from M/S Loba Chemie (Indo-Astranal Co. India) was used without further purification (bloom factor not known). It contained the following maximum nominal impurities: sulphate ash = 1.5%, $\text{SO}_2 = 2 \times 10^{-4}\%$ and heavy metals (Zn, Cu, Pb) in concentrations lower than the SO_2 concentration. This preparation was devoid of any *Escherichia coli* and liquifier. The gelatin sample had a narrow molecular weight distribution with a M_w peak at about 1.5×10^5 . Further details about the sample can be found in Ref. [8]. Aqueous GA stock solution (25%) was obtained from S. D. Fine-Chem, batch no. 0895-01-595-030811. To get a stable gel, four different solutions of varying GA concentrations [1×10^{-3} , 2×10^{-4} , 5×10^{-5} and $1 \times 10^{-5}\%$ (w/v)] were chosen, with the gelatin concentration of 5% (w/v) fixed for every sample. The solvent was prepared with double-distilled water. The pH of the solutions was maintained at 6.8 using a 0.1 M sodium phosphate buffer ($\text{Na}_2\text{HPO}_4 + \text{NaH}_2\text{PO}_4 \cdot 2\text{H}_2\text{O}$). All the solutions were prepared by dissolving gelatin in the buffer followed by heating for nearly 1 h at about 50 °C to remove history effects. When the gelatin dissolved completely, the required amount of GA was added and the mixture was stirred well for 0.5 h. The solutions were then ultracentrifuged for 1 h at 6000 rpm to remove dust. The clean solutions were then transferred directly to 5-ml cylindrical quartz scattering cells. All the samples looked transparent with a light-yellow hue. Prior to

QELS measurements, the solutions were allowed to equilibrate for 10–15 h at room temperature. The scattering measurements were carried out using a home-made scattering setup. It comprised a standard goniometer with the sample chamber thermostated to an accuracy of ± 0.1 °C. The excitation source was a He:Ne randomly polarized laser ($\lambda = 632.8$ nm) (Aerotech) delivering a power output of 15 mW. The intensity of the light scattered from the sample was measured by photon counting. To obtain good data, the counting rate was maintained at 10^4 – 10^5 counts per second. For the QELS studies we used an autocorrelator (BI-9000 AT, Brookhaven Instrument Corporation, USA).

Before making any measurement, the goniometer was calibrated using a dilute suspension of standard polystyrene latex solution (particle size about 90 nm). To carry out the experiment, one of the samples was heated and loaded into the scattering cell maintained at 60 °C and the correlogram was recorded. Next, the sol was allowed to cool to 50, 40 and 25 °C and the correlograms were recorded at these temperatures. To obtain data reproducibility, each experiment was performed 3 times. Each run took at least 30 min to give good signal statistics. This cycle was repeated for each sample. The correlation data were recorded down to the baseline. The background was estimated from the measured baseline statistics. Any correlation curve that showed a difference between the measured and calculated baseline greater than 0.1% was rejected. No curve had a signal modulation less than 50%.

Analysis of the QELS data

The normalized intensity autocorrelation function, $g_2(\tau)$, measured by the digital correlator can be related to the dynamic structure factor, $S(q, t)$, through the general expression [19]

$$g_2(q, t) = 1 + \beta' [2X(1 - X)S(q, t) + X^2|S(q, t)|^2], \quad (1)$$

where β' is the coherence area factor having a maximum value of 1. In a real experiment it defines the signal modulation which is a measure of the signal-to-noise ratio of the data. The parameter X ($0 \leq X \leq 1$) defines the extent of heterodyne contribution present in the measured $g_2(\tau)$ data. In the sol state $X = 1$ and the Siegert relationship, $g_2(\tau) = 1 + \beta'|S(q, t)|^2$, is established; however, in the gel state $X < 1$ and the term $2X(1 - X)$ makes a finite contribution to $g_2(\tau)$ and hence it must be accounted for. The value of X can be determined experimentally [19]. The intercept of the plot of $[g_2(q, t) - 1]$ versus delay time, t , at $t \rightarrow 0$ gives $\beta'[2X - X^2]$ from which the value of X can be calculated if β' is known. The estimation of $\beta' \leq 1$ which is an instrumental factor, can be done easily by performing an experiment at a high temperature where the system in the sol state shows zero heterodyne contribution. The variation of X with temperature is shown explicitly for one of our samples in Fig. 1. In the sol phase, we measured $X \sim 0.9$; hence, $S(q, t)$ could be determined from the $g_2(q, t)$ data directly, using the Siegert relation. In the gel phase, $X \sim 0.1$, and the prefactor of $S(q, t)$ in Eq. (1) is almost 20 times larger than the prefactor of $|S(q, t)|^2$. Thus we could neglect the contribution of the second term and fit the data to evaluate the various relaxation modes explicitly. The $g_2(\tau)$ data did not fit to a three-mode relaxation model (triple-exponential fitting) or to a single-exponential relaxation model. The best fit could be established where $S(q, t)$ was assigned a form

$$S(q, t) = Ae^{-\Gamma t} + Be^{-(t/\tau_c)^\beta} = S_f(q, t) + S_s(q, t), \quad (2)$$

where $S_f(q, t) = Ae^{-\Gamma t}$ and $S_s(q, t) = Be^{-(t/\tau_c)^\beta}$. In the sol state the $S(q, t)$ data points were evaluated from

$$S(q, t) = \{[g_2(q, t) - 1]/\beta'\}^{1/2} \quad (3)$$

and in the gel state from

$$S(q, t) = [g_2(q, t) - 1]/[2\beta'X(1 - X)]. \quad (4)$$

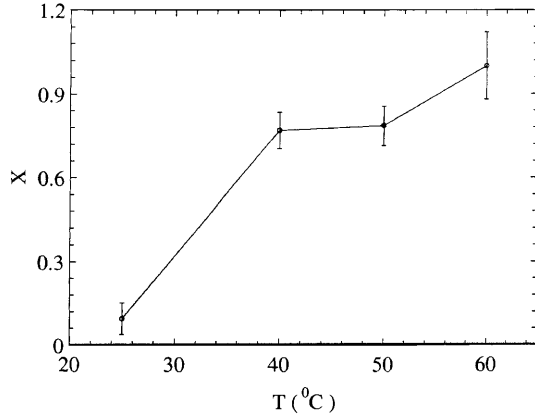


Fig. 1 Plot of the heterodyne contribution, X , as a function of temperature, T . The inversion point represents the gel point which was also confirmed on visual examination of all the samples at the transition temperature

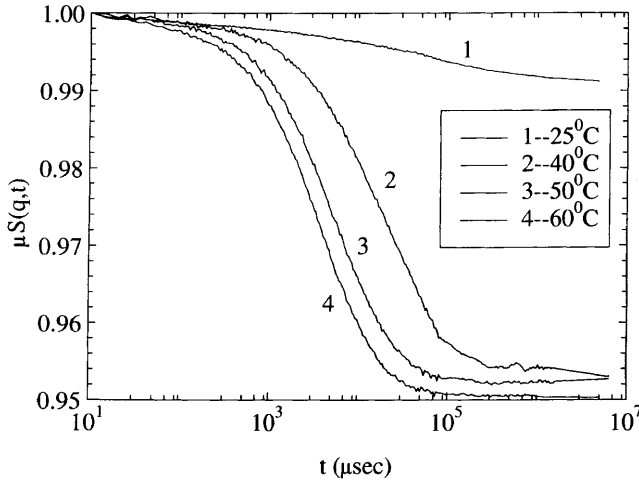


Fig. 2 The dynamic structure factor, $S(q, t)$, as a function of delay time, t , at four different temperatures above and below the gelation temperature of about 30°C for a sample of 0.001% (w/v) glutaraldehyde (GA) in 5% (w/v) gelatin prepared in phosphate buffer (0.1 M) maintained at a pH of 6.8

The evolution of $S(q, t)$ as the gel phase was approached can be observed in Fig. 2. Typical fits of the data to the fast and slow relaxation components of the $S(q, t)$ data are depicted in Figs. 3 and 4. The correlation data were split into two portions. For $t \leq 500 \mu s$, the correlation data were fitted to $S_f(q, t)$ and for $t \geq 500 \mu s$, the correlation data were fitted to $S_s(q, t)$.

Results and discussion

Fast-mode relaxation

The diffusion coefficient of the fast mode was deduced from $D_f = \Gamma_f/q^2$. The dependence of D_f on the concentration of the GA added is shown in Fig. 5, which

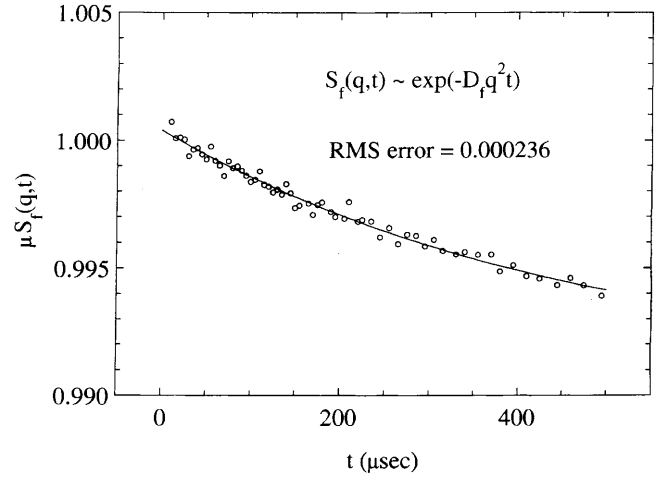


Fig. 3 The exponential regime of the structure factor, $S(q, t)$, for a solution of $5 \times 10^{-4}\%$ (w/v) GA mixed in 5% (w/v) gelatin and its fitting to $S_f(q, t) \sim \exp(-D_f q^2 t)$ (solid line). Excellent fitting for all of our samples was observed

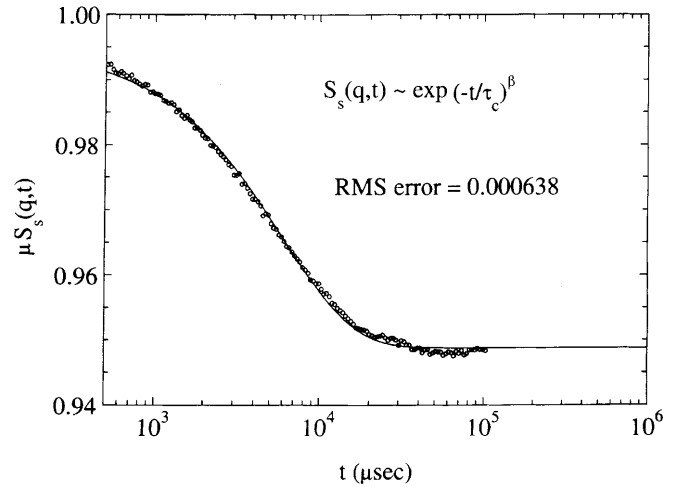


Fig. 4 The stretched exponential regime of the structure factor, $S(q, t)$, for a solution of $5 \times 10^{-4}\%$ (w/v) GA mixed in 5% (w/v) gelatin and its fitting to $S_s(q, t) \sim \exp(-(t/\tau_c)^\beta)$ (solid line). The fitting was to good accuracy for all our samples as evident from the root-mean-square (RMS) error of the fitting

implies a very weak dependence on the crosslinker concentration. At a given temperature, $D_f(c_T) \simeq D_0(1 + k_D c_T)$, with c_T being the total concentration (gelatin and GA). The interaction parameter $k_D = 2A_2M - k_f - \bar{v}$, where A_2 is the second virial coefficient of osmotic pressure, M is the polymer molecular weight, k_f is the concentration dependence of the frictional coefficient f of the network [i.e., $f = f_0(1 + k_f c_T)$] and \bar{v} is the partial specific volume of the polymer. According to the Flory-Huggins theory of polymer solutions [20], A_2 can be equated to

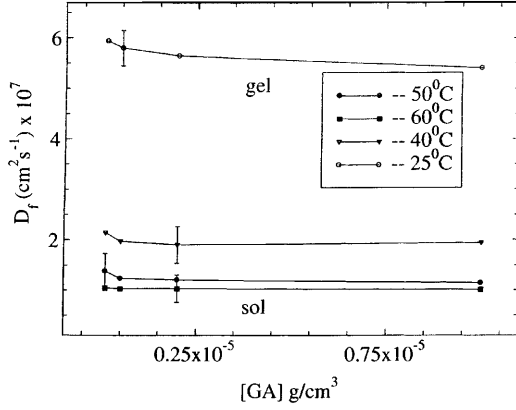


Fig. 5 The fast-mode diffusion coefficient, D_f , as a function of the concentration added GA for four different temperatures: 25, 40, 50 and 60°C. At a fixed temperature, D_f was independent of the concentration of added GA. There is a decrease in the fast-mode diffusion coefficient as the solutions evolved from sol to gel states (see text for details)

$$A_2 = \frac{\bar{v}}{V_1} (0.5 - \chi) , \quad (5)$$

where V_1 is the molar solvent volume and χ is the Flory–Huggins interaction parameter defining the solvent quality. The fast-mode diffusion is normally identified as the cooperative diffusion, D_c , or the gel-mode diffusion of the polymer network. The mesh size of the network can be deduced from [21]

$$D_f = D_c = \frac{k_B T}{6\pi\zeta\eta_0} , \quad (6)$$

where ζ is the average correlation length or mesh size of the constituent transient network. Since the GA concentration did not change significantly the D_f values, and consequently the ζ values, were independent of crosslinker concentration. The ζ values calculated for different temperatures are listed in Table 1. We observed a strong temperature dependence of the ζ values. Specifically, this implied shrinking of the network dimensions as the gel phase was approached. A better way to quantify the effect of GA concentration would be to estimate the crosslinking density in the solution at a given temperature. The Flory–Rehner equation [22] defines the ratio of the volume of the unswollen network to that of the swollen network at equilibrium ($v_e = 1/q_m$) as a characteristic crosslinking density parameter. Further, if M_e is the mass of the polymer between two entanglement points, for a good solvent the Flory–Rehner equation gives

$$q_m^{5/3} \cong (\bar{v}M_e)(1 - 2M_e/M)(0.5 - \chi)/V_1 . \quad (7)$$

Flory defined $(1 - 2M_e/M)$ as the network imperfection factor with an upper cutoff value of 1 for $M \rightarrow \infty$. In Eq. (7), approximately all the parameters except χ are

Table 1 Values of the heterodyne contribution factor, X , the width parameter β from a stretched exponential fitting of the dynamic structure factor data and the average mesh size, ζ , of the cross-linked network as a function of temperature, T . The mean value of β in the sol phase was 0.86 ± 0.06

T (°C)	X	β	ζ (nm)
25	0.1 ± 0.01	0.65 ± 0.09	3.8 ± 0.2
40	0.8 ± 0.03	0.80 ± 0.08	11 ± 1
50	0.8 ± 0.02	0.88 ± 0.03	18 ± 2
60	1.0 ± 0.02	0.93 ± 0.02	21 ± 2

independent of (or weakly dependent on) temperature. This allows us to write

$$q_m \sim (0.5 - \chi)^{3/5} . \quad (8)$$

If ξ_0 and ξ represent the mesh size of unswollen and swollen networks respectively,

$$q_m \sim (\xi/\xi_0)^3 . \quad (9)$$

Hence, combining Eqs. (8) and (9) one gets

$$\xi \sim \xi_0(0.5 - \chi)^{1/5} \quad (10)$$

or correspondingly, in terms of diffusion coefficients,

$$D_f \sim D_{f0}(0.5 - \chi)^{-1/5} . \quad (11)$$

Assuming an Arrhenius temperature dependence for D_0 , $D_0 \sim e^{(A/RT)}$, A being the appropriate activation energy of diffusion for the unswollen network, Eq. (11) reduces to

$$D_f \sim (0.5 - \chi)^{-1/5} e^{(A/RT)} . \quad (12)$$

Since, D_f was independent of GA concentration, it would not be wrong to assign χ the same temperature dependence that was measured for pure gelatin solutions, to a reasonably good approximation. We used the values of χ from Ref. [23] and fitted Eq. (12) to the data of Fig. 6. In Fig. 6 (inset), the y-axis has been normalized and least-squares fitted to Eq. (12). We obtained $A = (2863 \pm 3) \text{ J mol}^{-1}$. Hence, the mesh size showed a temperature dependence given by

$$\xi \sim (0.5 - \chi)^{1/5} e^{(-A/RT)} . \quad (13)$$

Since, $\Gamma_f = D_f q^2$ is a measure of the rate of relaxation of local concentration gradients, it can be attributed to the cooperative movement of entangled transient networks of polymer chains. It was argued earlier that as the temperature is reduced, the number of crosslinked chains increases [18]. This would make ξ decrease with temperature as observed in our studies. There is evidence of Γ_f showing just the opposite behaviour in the sol phase. The increase in the concentration of crosslinked chains was observed to reduce the Γ_f values in the sol phase. In the gel phase Γ_f showed no dependence on the concentration of crosslinked chains [18]. Our results are opposite to these observations. We attribute this

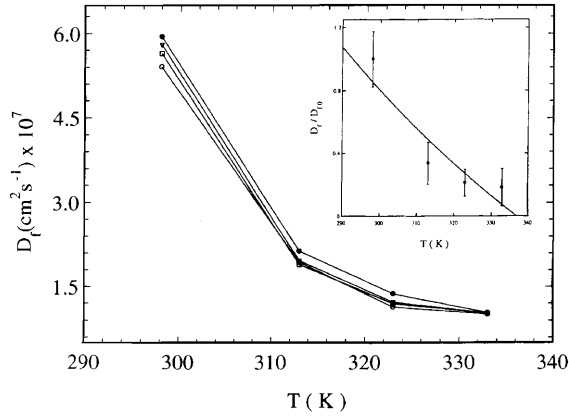


Fig. 6 The fast-mode diffusion coefficient, D_f , as a function of temperature T for four different concentrations of GA: $1 \times 10^{-3}\%$ (\circ), $2 \times 10^{-4}\%$ (\diamond), $5 \times 10^{-5}\%$ (∇) and $1 \times 10^{-5}\%$ (\bullet) (w/v). The inset shows the fitting of $D_f \sim (0.5 - \chi)^{-1/5} e^{(A/RT)}$ which gave the value of $A = (2863 \pm 3) \text{ J mol}^{-1}$. The solid lines are only to guide the eyes

discrepancy to the fact that these authors did not account for the heterodyne contribution to $g_2(\tau)$ and hence the reported Γ_f values were not representative of fast-mode relaxations. This was the case in most of the earlier studies.

Slow-mode relaxation

The slow-mode component of the dynamic structure factor, $S_s(q, t)$, was observed for $500 \mu\text{s} \leq t \leq 1 \text{ s}$. A typical fitting of the $S_s(q, t)$ data to a stretched exponential function $e^{-(t/\tau_c)^\beta}$ is shown in Fig. 4. The width of the relaxation time distribution function is given by β , which shows strong temperature dependence and no dependence on the concentration of the crosslinker GA. These β values are listed in Table 1 for different temperatures. The data could be fitted to (Fig. 7)

$$\beta(T) = \beta_0 + \beta_1 T + \beta_2 T^2, \quad (14)$$

the fitted values being $\beta_0 = 0.288$, $\beta_1 = 0.017$ and $\beta_2 = -1.07 \times 10^{-4}$.

Pure gelatin solutions yield $\beta = 0.75$ in the semidilute concentration regime [14]. For gelatin-sodium dodecyl sulphate complexes, β was measured to be 0.85 ± 0.09 in both sol and gel states of this polypeptide [17]. Ren and coworkers [15, 16] showed that for pure gelatin β had a value of 0.81 for the sol state and 0.67 for the gel state. Martin et al. [24] measured β to be 0.65 in gelling silica, which is a chemically crosslinked gel. The GA cross-linked gelatin system studied here conforms to these data quite well at 25 and 40 °C (Table 1). Ren and coworkers [15, 16] observed a sharp transition in the β versus temperature plot at the gelation temperature, T_{gel} . In comparison to this our β versus T plot was smooth (Fig. 7).

The relaxation time, τ_c , showed a strong dependence on the concentration of GA in the gel state but in the sol state there was no observable dependence. The dependence of τ_c on GA concentration is shown in Fig. 8. The data could be fitted to

$$\tau_c(c) = \tau_0 + \tau_1 c + \tau_2 c^2. \quad (15)$$

The fitted values were $\tau_0 = 7660 \pm 416$, $\tau_1 = (1.2 \pm 0.2) \times 10^7$ and $\tau_2 = (3.4 \pm 0.4) \times 10^{13}$ at 25 and 40 °C, i.e., the gel state, and $\tau_0 = 4915 \pm 187$, $\tau_1 = (0.9 \pm 0.1) \times 10^7$ and $\tau_2 = (0.95 \pm 0.27) \times 10^{13}$ at 50 and 60 °C, i.e., the sol state. The exact origin of the slow-mode relaxation is still unresolved. The existence of a slow mode in the sol phase has been pointed out by

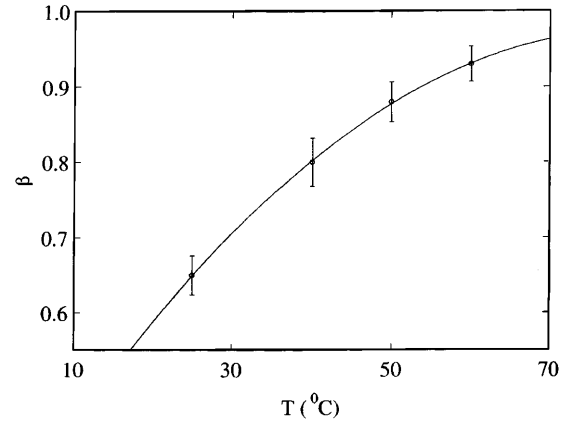


Fig. 7 The width exponent, β , of the stretched exponential fit of $S(q, t)$ as a function of temperature. The dotted line shows the fitting of β to $\beta(T) = \beta_0 + \beta_1 T + \beta_2 T^2$ and the fitted values are $\beta_0 = 0.288$, $\beta_1 = 0.017$ and $\beta_2 = -1.07 \times 10^{-4}$

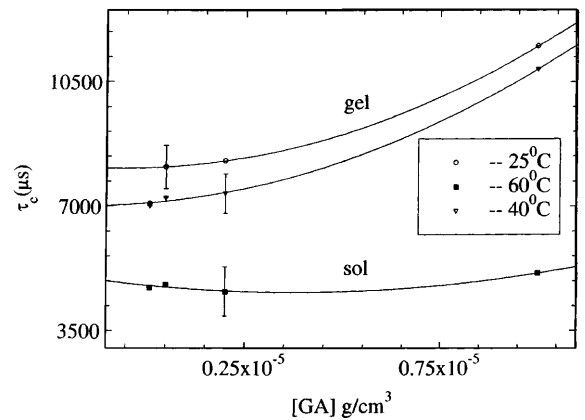


Fig. 8 Variation of the relaxation time, τ_c , as a function of GA concentration. In the sol state τ_c was found to remain independent of GA concentration, but it increased in the gel state. Fitting of τ_c to $\tau_c(c) = \tau_0 + \tau_1 c + \tau_2 c^2$ gave the values of $\tau_0 = 7660 \pm 416$, $\tau_1 = (1.2 \pm 0.2) \times 10^7$ and $\tau_2 = (3.4 \pm 0.4) \times 10^{13}$ at 25 and 40 °C, i.e., the gel state, and $\tau_0 = 4915 \pm 187$, $\tau_1 = (0.9 \pm 0.1) \times 10^7$ and $\tau_2 = (0.95 \pm 0.27) \times 10^{13}$ at 50 and 60 °C, i.e., the sol state

Borsali et al. [14], Amis et al. [10, 11] and Herning et al. [2] among others. Amis et al. [10, 11] and Herning et al. [2] attributed the presence of this slowly relaxing mode to the self-diffusion of a few polymer clusters through the rest of the solution. Such a description would be incompatible in a chemically crosslinked gel phase. Cho and Sakasita [25] observed the slow-mode relaxation frequency, Γ_s , showing a sharp discontinuity at T_{gel} . As mentioned earlier, these works did not account for heterodyning of the signal in the gel phase; thus the results for Γ_s invariably contain a finite amount of error. Borsali et al. [14] fitted a stretched exponential function to the $S_s(q, t)$ data and for the intermediate and concentrated gelatin solutions obtained an equivalent slow-mode diffusivity, D_s , which scaled with gelatin concentration, c , as

$$D_s \sim c^{-\alpha}, \quad (16)$$

with $\alpha = 1.31$ in the intermediate concentration regime and 2.73 in the concentrated regime, in close proximity to the 1.2 and 2.75 measured by Amis et al. [10, 11] for identical systems. In all these studies, the polypeptide chains were physically crosslinked as opposed to our case where both physical and chemical crosslinks were present.

A physical picture of this was provided by Oikawa and Nakanishi [18]. Here the total crosslink density, v_e , was assumed to be the sum of the chemical crosslinking density, $v_{e,\text{chem}}$, and the physical crosslinking density, $v_{e,\text{phys}}$. They calculated the values of $v_{e,\text{chem}}$ assuming the chemical crosslink sites to be tetra functional; however, in their description of the slow-mode dynamic structure factor they used $S_s(q, t) \sim e^{-\Gamma_s t}$, a formalism proved to be incorrect as we could not fit our data to a single-exponential function and had to use a stretched exponential fitting for $S_s(q, t)$. We can define the slow-mode diffusivity, D_s , as [17]

$$D_s = l^2/t_s = t_s^{\beta-1} \tau_c^{-\beta} q^{-2} \quad (17)$$

from purely dimensional considerations. Note that determination of D_s would necessitate a priori knowledge of t_s , which is unknown. Assuming the centre-of-mass diffusion of an imaginary particle of radius R , $D_s = k_B T / 6\pi\eta R$. Here $\eta = \eta_{\text{soln}}$ will yield self-diffusion and $\eta = \eta_{\text{solv}}$ the centre-of-mass motion in the solvent phase.

It is well known that for a self-diffusion process $D_s \sim T/\eta_{\text{soln}}$ and for the diffusion of a solute in a solvent medium $D_s \sim T/\eta_{\text{solv}}$ [20, 21]. Combining this with Eq. (17), a plot of $\ln(\eta_{\text{soln}}/T)$ versus $\ln\tau_c$ would yield a slope equal to β . Figure 9 shows a plot of $\ln(\eta_{\text{soln}}/T)$ versus $\ln\tau_c$ and the slope obtained was $\beta = 1.32 \pm 0.14$, in disagreement with the proposition of Eq. (17). We did not have the value of the solution viscosity and hence $\ln(\eta_{\text{soln}}/T)$ could not be plotted as was done by Ren et al. [16].

Conclusions

The chemically crosslinked gelatin solutions and gels showed two relaxation features. The normal fast-mode relaxation was attributed to the incipient gel mode arising due to short-range monomer or blob motion of the polypeptide chains, having a characteristic length, ξ , that showed strong temperature dependence (Fig. 10). In fact, the mesh size shrank at the onset of gelation.

The physical origin of the slow mode continues to be a matter of controversy. The anomalous diffusion model proposed by Havlin and Ben-Avraham [26] estimated the mean squared displacements, $\langle R^2 \rangle$, of the random walkers on a fractal lattice as

$$\langle R^2 \rangle = \begin{cases} l_1^2 \ln(t/t_1), & t < \tau_c \\ 2l_2^2(t/t_2)^\beta, & t \geq \tau_c \end{cases}, \quad (18)$$

where l_1, l_2 and t_1, t_2 are the elementary length and time steps of the random walks. There is a cutoff time, τ_c , below which the displacement grows logarithmically and

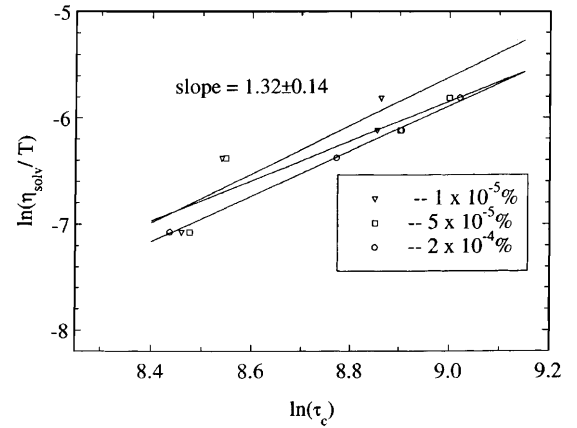


Fig. 9 Plot of $\ln(\eta_{\text{soln}}/T)$ versus $\ln\tau_c$ for solutions with different concentrations of added GA in gelatin [5% (w/v)]. A straight-line fit yielded a slope of 1.32 ± 0.14

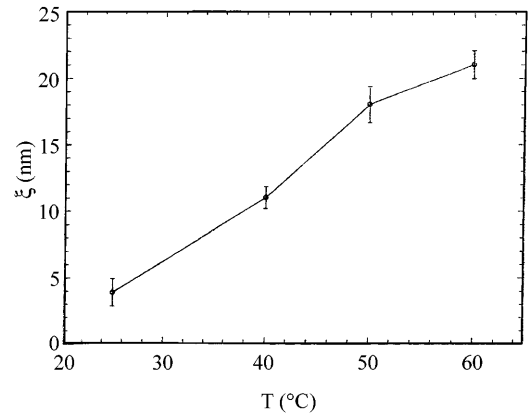


Fig. 10 Average mesh size, ξ , of the crosslinked network as a function of temperature, T . The solid line is only to guide the eye

above this there is power-law growth. Using a Gaussian diffusion model it can be shown that [16]

$$S(q, t) \sim \begin{cases} t^{-\alpha}, & t < \tau_c \\ e^{-(t/\tau_c)^\beta}, & t \geq \tau_c \end{cases} \quad (19)$$

We observed the $t \geq \tau_c$ behaviour exactly with stretched exponential functions both in sol and gel states.

When crosslinks are introduced into the polymer solution in large numbers, a three-dimensional interconnected network occurs, transforming the solution to a gel phase. The presence of the chemical crosslinks reduces the number of configurations originally accessible to the polymer chains in the dispersion medium. The equilibrium size of the network is decided by the balance between the osmotic force due to mixing of polymer and solvent molecules, which causes the gel to expand and an elastic force that tends to contract the network and expel the solvent. In such a situation the diffusion behaviour is expected to be strongly effected by local hydrodynamic forces acting on the polymer network. Hence, the Zimm model of polymer dynamics would be more appropriate for describing motions in our system. The Zimm model assumes that the polymer chain is a Gaussian chain with hydrodynamic interactions operating through the strings connecting the beads [27, 28]. Assuming a harmonic potential for these interactions, β was proved to be $2/3$.

Using the Gaussian chain approximation, the Rouse, Zimm and reptation models of relaxation have predicted the form of the dynamic structure factor to be [27–29]

$$S(q, t) = S(q, 0) \exp \left[- \left(\frac{t}{\tau_c} \right)^n \right], \quad (20)$$

where

$$n = \begin{cases} \frac{1}{2}; & \text{Rouse model} \\ \frac{2}{3}; & \text{Zimm model} \\ \frac{1}{4}; & \text{Reptation model} \end{cases} \quad (21)$$

and τ_c is the relaxation time for the model concerned. Accordingly, the stretched exponential mode of relaxation, i.e., $S(q, t) \sim e^{-(t/\tau_c)^\beta}$, should have a value of $\beta = 1/2$ for the Rouse dynamics, which is not true in our case. We found the value of $\beta = 0.86 \pm 0.06$ for the sol state and 0.65 for the gel state compared to 0.81 and 0.67 measured by Ren et al. [15, 16] for pure gelatin. Martin et al. [24] also measured the value of β to be 0.65 in the case of silica gels. Our value of β is close to the predictions of the Zimm model in the gel state. This cannot be attributed to the reptation model which predicts a much lower value of β .

The slow-mode relaxation frequency Γ_s , was reported to show a dip at T_{gel} . This was attributed to the minima of the elastic shear modulus at T_{gel} . Our measurements show smooth τ_c and β variations with temperature and we were unable to extract D_s explicitly from Eq. (17) due to reasons cited earlier.

Acknowledgement J.S. acknowledges financial support from the University Grants Commission, India.

References

1. Pezron I, Djabourov M, Leblond J (1991) *Polymer* 32:3201–3210
2. Herning T, Djabourov M, Leblond J, Takekart G (1991) *Polymer* 32:3211–3217
3. Pezron I, Herning T, Djabourov M, Leblond J (1990) In: Burchard W, Ross-Murphy SB (eds) *Physical networks, polymers and gels*. Elsevier, London, pp 231–254
4. Djabourov M (1991) *Polym Int* 25:135–143
5. Busnel JP, Morris ER, Ross-Murphy SB (1989) *Int J Biol Macromol* 11:119–125
6. Busnel JP, Ross-Murphy SB (1988) *Int J Biol Macromol* 10:121–124
7. Bohidar HB, Jena SS (1993) *J Chem Phys* 98:3568–3570
8. Bohidar HB, Jena SS (1993) *J Chem Phys* 98:8970–8977
9. Bohidar HB, Jena SS (1994) *J Chem Phys* 100:6888–6895
10. Amis EJ, Janmey PA, Ferry JD, Yu H (1983) *Macromolecules* 16:441
11. Amis EJ, Janmey PA, Ferry JD, Yu H (1981) *Polymer* 6:13
12. Brown W, Johnsen RM, Stilbs P (1983) *Polym Bull* 9:305
13. Chang T, Yu H (1984) *Macromolecules* 17:115
14. Borsali R, Durand D, Fischer EW, Giebel L, Busnel JP (1991) *Polym Networks Blends* 1:11–26
15. Ren SZ, Sorensen CM (1993) *Phys Rev Lett* 70:1727–1730
16. Ren SZ, Shi WF, Zhang UB, Sorensen CM (1991) *Phys Rev A* 45:2416–2422
17. Maity S, Bohidar HB (1998) *Phys Rev E* 58:729–737
18. Oikawa H, Nakanishi H (1993) *Polymer* 34:3358–3361
19. (a) Geissler E (1993) In: Brown W (ed) *Dynamic light scattering*. Clarendon, Oxford, pp 471–511; (b) Coviello T, Geissler E, Maier D (1997) *Macromolecules* 30:2008–2015
20. Flory PJ (1953) *Principles of polymer chemistry*. Cornell University Press, New York
21. De Gennes PG (1979) *Scaling concepts in polymer physics*. Cornell University Press, Ithaca
22. Flory PJ, Rehner J (1943) *J Chem Phys* 11:521
23. Bohidar HB (1998) *Int J Biol Macromol* 23:1–6
24. Martin JE, Wilcoxon J, Odinek J (1991) *Phys Rev A* 43:858–872
25. Cho M, Sakasita H (1996) *J Phys Soc Jpn* 65:2790–2792
26. Havlin S, Ben-Avraham D (1987) *Adv Phys* 36:695
27. Doi M, Edwards SF (1986) *The theory of polymer dynamics*. Clarendon Press, Oxford
28. Yamakawa H (1971) *Modern theory of polymer solutions*. Harper and Row, New York
29. Ebert U, Baumgartner A, Schaefer L (1997) *Phys Rev Lett* 78:1592–1595